RSC Advances

# Paper substrate modification for rapid capillary flow in microfluidic paper-based analytical devices



| | |
|---|---|
| Journal: | *RSC Advances* |
| Manuscript ID: | RA-ART-01-2014-000434 |
| Article Type: | Paper |
| Date Submitted by the Author: | 16-Jan-2014 |
| Complete List of Authors: | Xu, Yinchao; University of Tsukuba, Department of life and environmental sciences<br>Enomae, Toshiharu; University of Tsukuba, Department of life and environmental sciences |
| | |

Journal Name

RSCPublishing

ARTICLE

# Paper substrate modification for rapid capillary flow in microfluidic paper-based analytical devices

Cite this: DOI: 10.1039/x0xx00000x

Received 00th January 2012,
Accepted 00th January 2012

DOI: 10.1039/x0xx00000x

www.rsc.org/

Y. Xu[a] and T. Enomae[a]

The development of microfluidic paper-based analytical devices is the most promising emerging research globally, due to its main advantage of spontaneous liquid transport. Though many fabrication and detecting methods have been developed, there remain several challenges to overcome. In this paper, we present the findings of a simple and quick fabrication method that was developed by printing a modified poly(styrene-co-acrylic acid) solution using an ink jet printer. The formed hydrophobic barrier was then analyzed using a confocal laser scanning microscope and a scanning electron microscope. To overcome the problem of liquid analyte evaporation during long-distance delivery and long-time analysis, experiments were conducted on various conventional parameters in papermaking processes. To examine the influence of internal channel width, fiber orientation, plasma-etching treatment, beating degree and calendering, volumetric flow rates of channels were measured using an automatic scanning absorptometer. Consequently, internal channel width had no effect on the flow rate, and channels aligned along the machine direction exhibited higher volumetric and longitudinal flow rates than they did in the cross direction. Plasma-etching treatment was found to increase the longitudinal flow rate, but the volumetric flow rate remained virtually the same. It was also found that higher beating degrees decreased the flow rates, likely caused by the decreased radius of pores between fibers. Finally, it was found that calendering affected the flow rates only marginally.

Journal Name RSCPublishing

ARTICLE

## Introduction

Paper is a traditional material conventionally used for writing, printing and packaging. New and innovative research aimed at expanding the usesof paper continues to be pursued, resulting in various successful applications in a wide range of fields.

Since 2007, development of microfluidic paper-based analytical devices, as a growing field of research, have provided novel systems for fluid handling and fluid monitoring as well as food quality testing, due to its significant advantages including low-cost, spontaneous liquid transport based on capillary force, and compatibility with chemical/biochemical applications[1]. Moreover, cellulose fibers can be functionalized to change properties such as permeability and reactivity[2]. Up to now, most published research articles on paper-based devices have focused on the pursuit of low-cost and simple fabrication methods and on investigating new applications[3]. Several fabrication methods have been published and, based on the binding states of hydrophobic agents to paper, the paper patterning principles of the various techniques can be divided into three categories[1]: physical blocking of the pores in paper, such as photolithography[4, 5, 6], analogue plotting[7] and laser treatment[8, 9]; physical deposition of a hydrophobizing reagent, such as wax printing[10, 11, 12], flexography printing[13] and screen printing[14]; and chemical modification of fiber surfaces, such as ink jet printing[15] and plasma treatment[16, 17].

Even though paper is a promising alternative substrate for analytical sensors, there are still some limitations that have been reported. One of the main limitations is low liquid sample retention, i.e., idle sample consumption within paper fluidic channels and the sample evaporation during transport, resulting in low efficiency of sample delivery within the device[3]. However, this limitation has not drawn much attention.

Conventional research on liquid transport in paper has usually been conducted uniquely for particular applications such a sink penetration in printing, or the spread of an aqueous ink over a paper surface in ink jet printing. Moreover, no universal theory of fluid transport can possibly cover all of the different end-use applications of paper[18]. For the one-dimensional flow in a porous matrix like a paper strip, the fluid flow follows the Lucas-Washburn equation[19]. Z. W. Zhong et al. had mainly studied the effect of width of a channel by recording the distance travelled with time using a video camera[20]. However, little research has been under taken to explore substrate characteristics for paper-based sensors.

Therefore, the investigation discussed here was pursued with a view to developing a simple channel fabrication method using ink jet printing technology, and then analyzing the resulting formed hydrophobic barrier. Furthermore, properties of paper substrates required to improve the delivery rate of a liquid analyte were examined from representative parameters of papermaking processes by measuring the rate of water absorption through channels, which could assist in selecting or designing the most suitable paper substrate for further complex paper sensor fabrication.

## Experimental

### Preparation of PS-co-PAA ink

Poly(styrene-co-acrylic acid), or PS-co-PAA, is a popular internal sizing agent in the papermaking industry for the hydrophobization of paper. In this work, a solution of PS-co-PAA (CP-900, Harima Chemical) was used as an ink to fabricate a channel on paper. This chemical was modified in the following way so that it would be suited well to ink jet printing. First, the original PS-co-PAA solution was diluted with water at a PS-co-PAA to water ratio of 1:10. Then, the diluted solution was mixed with ethylene glycol at a diluted PA-co-PAA to EG ratio of 3:7 to prevent head nozzles from being clogged by PS-co-PAA when it dried. Approximately 1 % Neutral red was added for improved visualization of hydrophobic barriers and analysis using confocal laser scanning microscope after no adverse effect of Neutral red was observed in micrographs.

### Preparation of the paper substrate

Filter paper (No.1, Advantec) was used in the experiments to examine the effects of channel width, fiber orientation and plasma-etching treatment. Laboratory sheets were prepared for examining the effects of beating and calendering.

The Filter papers used in the experiment for examining plasma-etching were treated in two plasma-etching modes using a plasma ion bombarder (PIB, Shinku riko) as shown in Table 1.

The laboratory sheets were prepared from hardwood bleached kraft pulp (HBKP) (Oji Paper Co., Ltd., Japan) beaten to various beating revolutions (2000, 5000 and 10000 rev) using PFI mill. Canadian Standard Freeness (CSF) was measured according to ISO 5267-2:2001. The laboratory sheets were also prepared with no additives, according to ISO 5269-1:2005. Structural parameters including grammage and thickness were measured according to ISO 536:2012 and ISO 534:2011, respectively and the density was calculated by dividing grammage by thickness.

For calendering, rectangular samples with a length of 120 mm and a width of 100 mm were cut using a guillotine cutter from the laboratory sheets prepared from a HBKP beaten to 2000 rev. The samples were calendered at different calendering pressures (0.5 and 1MPa) using a laboratory calender (No.2232, KRK, Japan) equipped with a nip of steel and neoprene rubber rolls speed of 3.5 m/min. The surface temperature steel roll was approximately 60 °C. Before and after calendering, the grammage and thickness of the samples were measured and the density was calculated.

For plasma-etching, 2 modes were applied as shown in Table 1.

Table 1. Parameters of two plasma-etching conditions

| Mode | Vacuum (Pa) | Current (mA) | Time (min) |
|---|---|---|---|
| Hydrophilization mode | 20 | 20 | 2 |
| PDMS (polydimethylsiloxane) mode | 80 | 30 | 2 |

### Channel fabrication by ink jet printing

Channels were fabricated using an ink jet printer (Dimatix DMP-2831, Fujifilm). Since micro-droplets of the ink ejected from the head nozzle are quite tiny (10 picoliter/droplet), one-time printing could not provide a sufficient volume of PS-co-PAA ink to make a continuous barrier that would penetrate the paper completely to the backside, thereby fabricating a channel with no defects. In this case, overlap printing was needed, and the printing times were adjusted according to the paper substrates.

### Characterization of the channel structure

Since Neutral red has a fluorescence property, hydrophobic barriers were observed using a Confocal Laser Scanning Microscope (CLSM) (LSM 710, Carl Zeiss) and 3D images were produced[21].

A Scanning Electron Microscope (SEM) (S-4200, Hitachi) was used to identify the PS-co-PAA distribution in the paper substrate. A small area of filter paper with a length of 10 mm and a width of 8 mm,

with a channel fabricated by different times of overlap printing, was cut out and affixedto an aluminum specimen stub using conductive tape. The test sample was then treated with a Pt-Pd alloy coating using an ion sputter (E1030, Hitachi) for 250s once the vacuum reached 6 Pa. This was done to provide electrical conductivity in the sample .Then, the sample was observed using the SEM.

**Water absorption test**

**Channel design**

First, to examine the effect of fiber orientation on flow rates, channels with lengths of 40 mm and widths of 4 mm were aligned lengthwise in both the machine direction (MD) and the cross direction (CD) of the filter paper. Secondly, to examine the effect of plasma-etching treatment, channels with lengths of 40 mm and widths of 4 mm were fabricated along the MD in the filter paper. Thirdly, channels with the same length of 40 mm and different widths of 3, 4, or 5 mm were tested as well to investigate the effect of the channel width. To measure the practical width of channels, pictures of a certain length of channels with an identified scale were taken using a digital camera (C3040ZOOM, Olympus) mounted on the stereo microscope (SZX10, Olympus) after the channel inside was stained with an aqueous solution of Nile blue. The blue area and length of channels in the pictures were measured using ImageJ, which is a Java-based image processing program developed at the National Institute of Health (http://rsb. info. nih. gov/ij/). The average width was calculated by dividing the area by the length. The total length measured per channel was about 30 mm, which was approximately three quarters of each channel.Then, those channels with lengths of 20 mm and widths of 4 mm were also fabricated to examine the effect of beating. Finally, to examine the effect of calendering pressure, rectangular channels with lengths of 20 mm and widths of 4 mm were fabricated on calendered laboratory sheets and tested.

Before each water absorption test, commercial adhesive tape (CM-12, Scotch) was affixed to the backside of each channel to prevent water leakage, and no water would be absorbed by the tape. It should be noted that the adhesive tape was proven to have no influence on water absorption by the Klemn method, which is often used for determining water absorbency of paper slips as a water rise by capillary force for the specified time after immersing the slip end to the specified depth in water. The volume of water absorbed into a channel over time was measured with an Automatic Scanning Absorptometer (ASA) (KumagaiRiki Kogyo). The water supply head was placed on one end of a channel and kept at the same location. As water penetrated the channeland travelled toward the oppositeend, the amount of water absorbed was recorded with time and displayed on a computer. Each measurement was discontinued as soon as the front edge of the water flow reached the oppositeend. Fig. 1 shows an example of the ASA test.

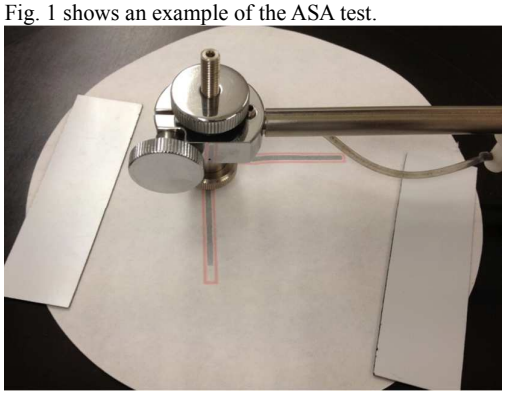

Fig. 1 Water absorption test with channels using ASA.

The speed at which water is absorbed by volume, and the average flow speed in distance that can be calculated by dividing the channel length by the total testing time, will be referred to as "volumetric flow rate" and "longitudinal flow rate", respectively hereafter. The former is more important for a sensing test in need of a certain large volume of a liquid analyte such as a multicomponent analysis, and the latter is more important for a quick test.

To analyze the results for one condition, regression analysis was applied to every curve of each test. To summarize several (at least 5 times) absorption measurements in one condition, the average regression curve was calculated.

Thus, the data point at the end of each curve, which represents the average time and volume of water absorbed, also included error bars designating a 95% confidence interval. The error bar of y-axis indicates the 95% confidence intervals of the total volume absorbed into the channel in each test. And the error bar of x-axis indicates those of the time consumed in each test.

**Total pore volume of channels**

The total pore volume of each channel, which indicates the capacity of containing water, was calculated by assuming that a paper substrate contains an air-occupied pore layer and a fiber layer as shown in Fig. 2, although for all intents and purposes, they are practically mixed.

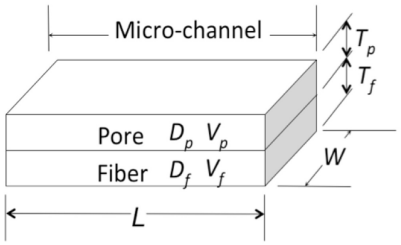


Fig. 2. Schematic diagram of a channel by assuming the paper sheet comprises a pore layer and a fiber layer.

The total volume $V$ of a channel equals the sum of the total pore volume $V_P$ and the total fiber volume $V_f$:

$$V = V_P + V_f \quad (1)$$

The total thickness $T$ equals the sum of the pore layer thickness $T_p$ and the fiber layer thickness $T_f$:

$$T = T_p + T_f \quad (2)$$

Then, the grammage of the paper substrate $B$ equals the mass of the two layers divided by the area:

$$B = \frac{T_p LW D_p + T_f LW D_f}{LW}, \quad (3)$$

Where $L$ and $W$are the length and width of the channel, respectively. Therefore, pore volume can be calculated by assuming the density of cellulosic fibers to be 1500 kg/m$^3$:[22]

$$V_p = V - V_f = TLW - T_f LW = TLW - \frac{BLW}{D_f} = (T - \frac{B}{1500})LW \quad (4)$$

## Results and Discussion

**Channel structure**

Fig. 3 shows that a sufficient amount of solution (by overlap printing) was used to penetrate the paper in the direction of its thickness in order to fabricate effective barriers.

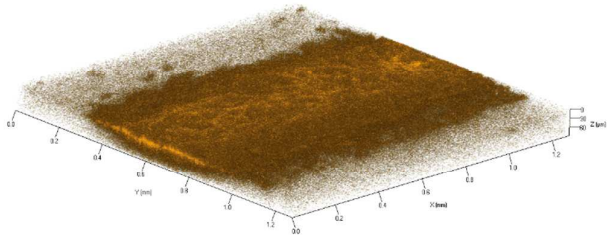

Fig. 3.Three-dimensional image of a section of a hydrophobic barrier.

Fig. 4 shows that the cross-sectional area increased with greater number of printing times.The PS-co-PAA ink penetrated in the sheet of paper transversely to form ahydrophobic barrier, and the barrier width increased due to largerlateral spread and penetration of the ink as the printing times increased. This was observed even for barriers

with the same designed width.

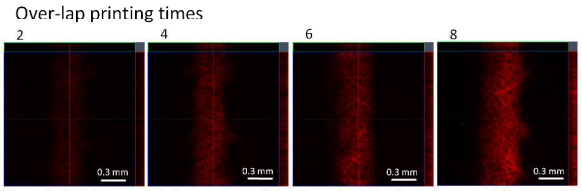


Fig. 4 Orthogonal images of hydrophobic barriers with a width of 0.3 mm at different overlap printing times.

Fig. 5 shows film-like PS-co-PAA that was observed to attach to fiber surfaces and particles, which was identified to be Neutral red separated out of the ink after drying.
PS-co-PAA was found to turn filmy separately from Neutral red particles and cover fiber surfaces partially. Pieces of hydrophobic material scattered but located closelyrepel water well by the lotus effect.[23]

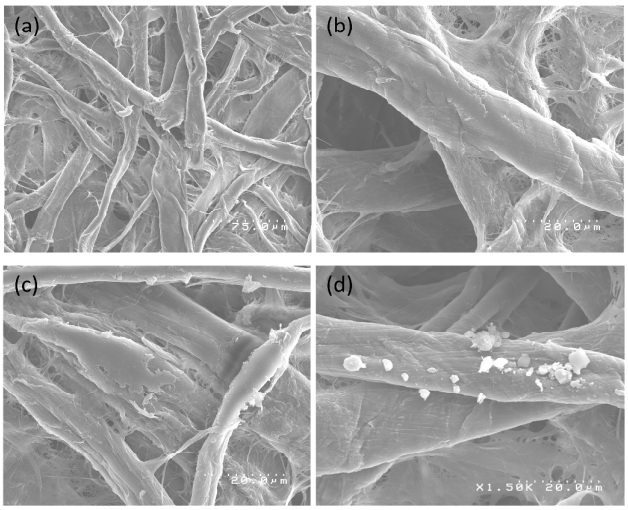


Fig. 5. SEM images of hydrophilic and hydrophobic areas in paper:(a) (b) untreated paper at different magnifications, (c) Film (PS-co-PAA) and (d) particles (Neutral red) in printed hydrophobic areas.

**Parameters affecting water flow rate**

**Channel width**

As discussed in the previous section, the width of the hydrophobic barrier increased due to the overlap printing, which resulted in a narrower real channel width compared to the designed channel width. The channel widths were measured to be 2.161, 3.529 and 4.359 mm, although the designed widths were 3, 4 and 5 mm, respectively.

After being normalized with measured channel width, Fig. 6 shows that the internal width of a channel had almost no influence on the volumetric flow rate per unit width. The longitudinal flow rate that is inversely proportional to the time indicated at the final data point of each curve was also significantly the same. This result suggests that the channel width could be designed depending on the volume of analyte required for each test.

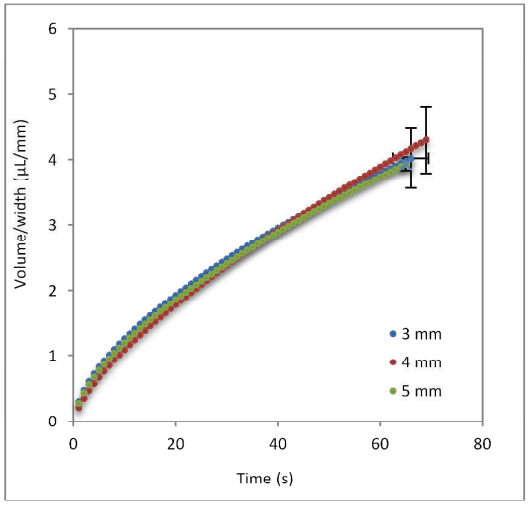


Fig. 6 Comparison in volume of water absorbed per unit width in channels with different widths fabricated in filter paper.

**Fiber orientation and plasma-etching treatment**

Fig. 7 clearly shows that a channel aligned in MD produced higher volumetric and longitudinal flow rates than that aligned in CD. In machine-made papers, there are more fibers aligned in MD than in CD. Fiber orientation refers to this anisotropy in the structure of paper. It is caused by the friction between fibers and a forming wire in a paper machine.

Water in paper is known to penetrate according to the Lucas-Washburn equation. Fiber alignment controls pore radius and capillary distribution. As a network model, the mean radius of pores between fibers is not much different between MD and CD, but the tortuosity of capillaries is considered to be much greater in MD than in CD. For quick liquid transport, therefore, microfluidic paper should be produced with a high fiber orientation degree so that the direction of fiber orientation will be in parallel to the longitudinal direction of the channel.

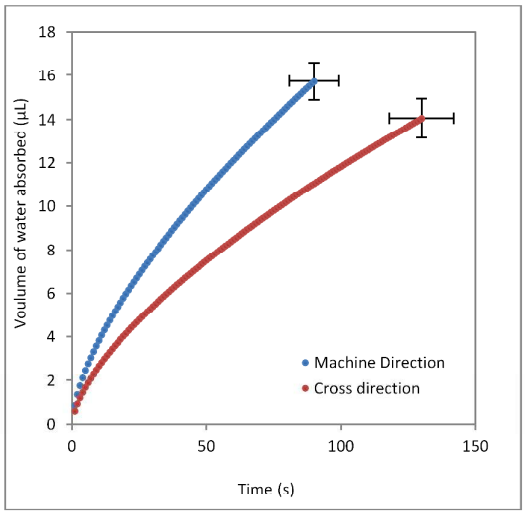


Fig. 7. Comparison of volume of water absorbed in channels fabricated along MD and CD.

Fig. 8 shows that with the etching treatment, the volumetric flow rate increased in the hydrophilization mode and decreased in the PDMS mode.Therefore, the overall volumetric flow was only marginally affected. On the other hand, the longitudinal flow rate slightly increased. This finding suggests that plasma-etching treatment is also a functional method to improve the longitudinal flow rate of a channel.

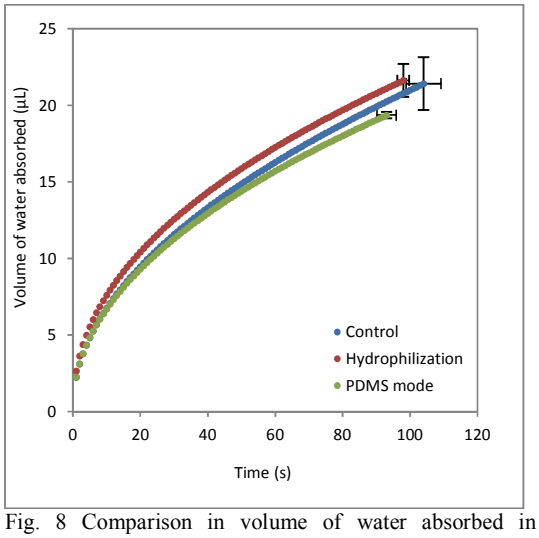


Fig. 8 Comparison in volume of water absorbed in channels fabricated in filter paper treated in different etching modes.

**Beating degree**

Beating with PFI mill refers to the mechanical action to fibers between rotating bars and a stationary smooth-walled housing. The major effect is raising fine fibrils on the surfaces of beaten fibers and providing fiber flexibility, resulting in a remarkable increase in surface area for forming more hydrogen bonds and greater contact area between fibers. Thus, this tight bonding leads to not only higher paper strength but also a smaller pore size among fibers.

Fig. 9 shows the original data from the ASA, illustrating the volume of water absorbed overtime and how it was affected by different beating degrees. The data were normalized by dividing by the grammage of each paper sample, as shown in Fig. 10. Table 2 and Fig. 10 also show that laboratory sheets with lower densities (lower beating degrees) were considered to have larger pore size and therefore provided higher volumetric and longitudinal flow rates, which is consistent withthe Lucas-Washburn equation. However, laboratory sheets with smaller pore size (higher beating degrees) absorbed larger volumes of water at the end of the channel, presumably due to fiber swelling during the long time test.

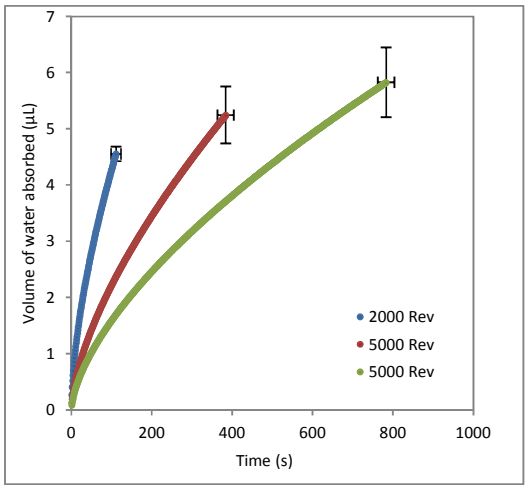


Fig. 9 Comparison of volume of water absorbed into channels fabricated in handsheets with different beating degrees.

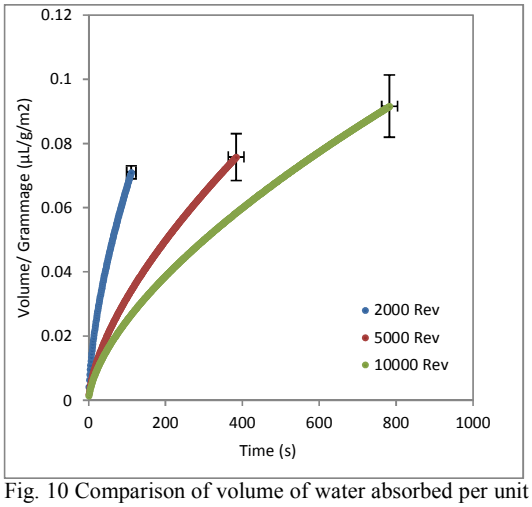


Fig. 10 Comparison of volume of water absorbed per unit grammage into channels fabricated in handsheets with different beating degrees.

Table 2. Canadian Standard Freeness (CSF) of beaten pulps and structural parameters of laboratory sheets

| Beating revolutions | 2000 | 5000 | 10000 |
|---|---|---|---|
| CSF (ml) | 525 | 482 | 371 |
| Grammage (g/m$^2$) | 64.1 | 69.2 | 63.6 |
| Thickness (µm) | 95 | 96 | 83 |
| Density (kg/m$^3$) | 675 | 720 | 766 |

**Calendering**

Fig. 11 shows the data from the ASA, illustrating the water absorption volume overtime and how it was affected by calendering. Table 3 shows that density increased as calendering pressure increased. Together, Fig. 10 and Table 3show that the volumetric flow rate increased to a certain degree (although the longitudinal flow rate decreased slightly) with increased paper density due to the increased calendering pressure. Consequently, it was found that smaller total pore volume resulted in higher total absorption volume, presumably because no hydrogen bonding was formed during calendering unlike beating and compressed fibers recovered quickly or sprang back to their original status during water penetration. Even after calendering, the original fiber network seems more dominant. This recovery effect, therefore, was significant and diminished the difference among the three samples, as shown by the marginal differences. In summary, calendering hardly affected the volumetric water flow rate or longitudinal flow rate.

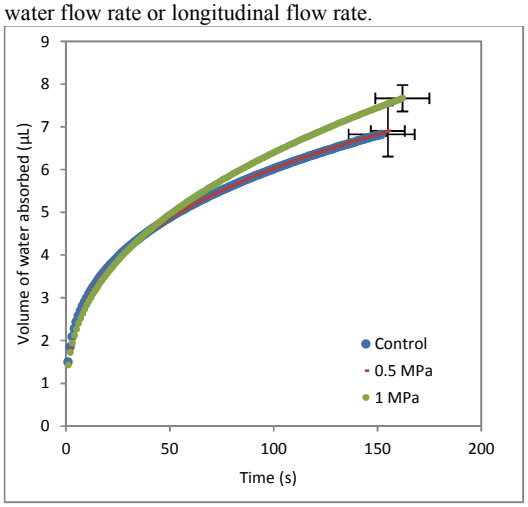


Fig. 11 Comparison of volume of water absorbed into channels fabricated in handsheets,calendered at different pressures.

Table 3.Calendering and structural parameters of laboratory sheets

| Sample No. | | 1 | 2 | 3 |
|---|---|---|---|---|
| Pressure (MPa) | | Uncalendered | 0.5 | 1 |
| Grammage (g/m$^2$) | | 62.8 | 66.5 | 64.2 |
| Before calendering | Thickness (μm) | 89 | 94 | 93 |
| | Density (kg/m$^3$) | 706 | 711 | 693 |
| | Total Pore Volume (μL) | 6.78 | 7.17 | 7.10 |
| After calendering | Thickness (μm) | 89 | 91 | 85 |
| | Density (kg/m$^3$) | 706 | 730 | 747 |
| | Total Pore Volume (μL) | 6.78 | 6.93 | 6.46 |

## Conclusions

By undertaking this research, it was proved that printing PS-co-PAA ink using an ink jet printer is a feasibleway to fabricate hydrophobic barriers of channels for aqueous liquid delivery in paper substrates. This technique is expected to contribute to the creation of paper-based sensors simply and efficiently at low costs.

Channel width had no effect on the longitudinal flow rate, suggesting that the volumetric flow rate is proportional to the channel width. A channel aligned in MD had higher volumetric and longitudinal flow rates than that aligned in CD. Plasma-etching treatment was shown to increase the longitudinal flow rate due to higher wettability of fiber surfaces. Beating increased paper density and reduced both volumetric and longitudinal flow rates likely due to reduced pore size. Calendering had a minimal effect on the volumetric or longitudinal flow rates. The channel response to water was different between the beating and calendaring papermaking processes. Pore size in paper substrates and hydrogen bonding formation during the process were found to be important parameters.

Finally, channels fabricated on paper substrates prepared from less beaten pulp and along MD of the paper, regardless of calendering degrees, are considered to be advantageous for a higher longitudinal flow rate to save time in microfluidic paper-based sensing tests. In addition, from the perspective of paper science, the conclusions are universal for paper without special treatment.

## Acknowledgements

The authors would like to thank Harima Chemicals Group, Inc. for supplying the sizing agent CP-900, Shinku riko Co., Ltd for supplying the plasma ion bombarder, and Oji Paper Co., Ltd. for supplying hardwood bleached kraft pulp.

## Notes and references

[a]Department of Life and Environmental Sciences, the University of Tsukuba, Tennodai 1-1-1, Tsukuba, Ibaraki 305-8572, Japan

1. X. Li, D. R. Ballerini and W. Shen, *Biomicrofluidics*, 2012, **6**, 011301.
2. P. J. Bracher, M. Gupta and G. M. Whitesides, *J. Mater. Chem.*, 2010, **20**, 5117-5122.
3. D. D. Liana, B. Raguse, J. J. Gooding and E. Chow, *Sensors*, 2012, **12**, 11505-11526.
4. A. W. Martinez, S. T. Phillips, M. J. Butte and G. M. Whitesides, *Angrew. Chem. Int. Ed.*, 2007, **46**, 1318-1320.
5. A. W. Martinez, S. T. Phillips and G. M. Whitesides, *Proc. Natl. Acad. Sci.*, 2008, **105**, 19606–19611.
6. S. A. Klasner, A. K. Price, K. W. Hoeman, R. S. Wilson, K. J. Bell and C. T. Culbertson, *Anal. Bionanl. Chem.*, 2010, **397**, 1821–1829.
7. D. A. Bruzewicz, M. Reches and G. M. Whitesides, *Anal. Chem.*, 2008, **80**, 3387–3392.
8. A. W. Martinez, S. T. Phillips, G. M. Whitesides and E. Carriho, *Anal. Chem.*, 2010, **82**, 3–10.
9. G. Chitnis, Z. W. Ding, C. L. Chang, C. A. Savran and B. Ziaie, *Lab Chip*, 2011, **11**, 1161–1165.
10. Y. Lu, W. W. Shi, L. Jiang, J. H. Qin and B. C. Lin, *Electrophoresis*, 2009, **30**, 1497–1500.
11. V. Leung, A. A. M. Shehata, C. D. M. Filipe and R. Pelton, *Colloid. Surf. A: Physicochem. Eng. Asp.*, 2010, **364**, 16–18.
12. Z. W. Zhong, Z. P. Wang and G. X. D. Huang, *Microsyst. Technol.*, 2012, **18**, 649–659.
13. J. Olkkonnen, K. Lehtinen and T. Erho, *Anal. Chem.*, 2010, **82**, 10246–10250.
14. W. Dungchai, O. Chailapakul and C. S. Henry, *Analyst.*, 2011, **136**, 77–82.
15. M. S. Khan, D. Fon, X, Li, J. Tian, J. Forsythe, G. Garnier and W. Shen, *Colloid. Surf. B: Biointerfaces.*, 2010, **75**, 441–447.
16. X. Li, J. Tian and W. Shen, *Cellulose*, 2010, **17**, 649–659.
17. X. Li, J. Tian, T. Nguyen and W. Shen, *Anal. Chem.*, 2008, **80**, 9131–9134.
18. M. Leskelä and S.Simula, in *Papermaking Science and Technology*, ed. J. Gullichsen and H. Paulapuro, FapetOy,Finland, 1st edn., 1999, Vol. 16,ch. 9, pp:285-286.
19. E. Fu, B. Lutz, P. Kauffman and P. Yager, *Lab Chip*, 2010, **10**, 918-920.
20. Z. W. Zhong, Z. P. Wang and G. X. D. Huang, *Microsyst. Technol.*, 2012, **18**, 649-659.
21. T. Enomae, M. Naito, A. Isogai, Y. Ozaki, and H. Nagashima, *J. Imaging Sci. Technol.*, 2011, **55**, 020201 1–8.
22. L. J. Gibson, *Journal of Royal Society Interface,* 2012, **9**, 2749–2766.
23. K. Jia, H. H. Zhang, X. Q. Fan, X. P. Jiang, and S. Liu, *Key Engineering Materials*, 2007, **339**, 252–256.

 